RSC Advances

ROYAL SOCIETY OF CHEMISTRY

www.rsc.org/advances

CdS nanoparticles anchored on the surface of yeast via hydrothermal processes for environmental applications

Fang Qin [a], Bo Bai*[, b, a], Dengwei Jing [c], Lan Chen [a], Rui Song [a], Yourui Suo [b]

[a] College of Environmental Science and Engineering Chang'an University, Xi'an,
710054, P.R. China

[b] Northwest Plateau Institute of Biology, Chinese Academy of Sciences , Xining,
810001, P.R. China

[c] International Research Centre for Renewable Energy & State Key Laboratory of
Multiphase Flow in Power Engineering, Xi'an Jiaotong University, Xi'an,
Shaanxi 710049, P. R. China

* Corresponding author

Email address: baibochina@163.com

Tel: +86 29 82339052

Fax: +86 29 82339961

Abstract: Cadmium sulfide (CdS) nanoparticles were successfully anchored on the surface of yeast via a hydrothermal process, forming fructus rubi-like CdS@yeast hybrid microsphere. In this method, the innate functional groups inherited from the hydrophilic cell wall of microbial cells were utilized to anchor Cd^{2+} ion, and then the CdS@yeast hybrid particles with fructus rubi-like morphology were obtained in the presence of thioacetamide (TAA) by a hydrothermal treatment process. The products were characterized by scanning electron microscopy (SEM), confocal laser scanning microscope (CLSM), powder X-ray diffraction (XRD) and UV-Vis diffuse reflectance spectra. The sedimentation performance of CdS@yeast microspheres in aqueous solutions was evaluated to demonstrate the unique features of CdS@yeast in comparison with bulk CdS nanoparticles. The interaction between host core yeast and guests CdS nanoparticles was investigated by fourier transform infrared (FT-IR) spectroscopy and the possible mechanisms for formation of CdS@yeast hybrid microspheres were proposed. The model photocatalytic test showed that the fructus rubi-like CdS@yeast microsphere could efficiently remove metylene blue (MB) dyes from aqueous solutions due to the combined functions from the bio-sorption of the yeast core and photocatalytic degradation driven by the attached CdS nanoparticles. The present approach represents a guide for the preparation of a variety of hybrid composites with similar structure for treatment of the toxic organic pollutants.

Keywords: CdS@yeast; Hydrothermal; Hybrid Nano-materials; Dyes;

1. Introduction

The hybrid particles have become one of the most effective sources for advanced materials because they usually exhibit enhanced and even novel properties (e.g., mechanical, chemical, electrical, rheological, magnetic, and optical) in comparison with traditional composites [1-2]. For instance, the unique surface configuration or heterogeneous textural characterization of hybrid composites have revealed substantially different properties from that of their own host core or guest particle, such as different surface chemical composition, increased stability, and different magnetic or optical properties [3]. In return, these properties make the hybrid composites suitable for a wide range of potential applications including surface enhanced Raman scattering (SERS) [4], catalysis [5], non-linear optics [6], bio-analysis [7], and capsules for controlled release of therapeutic agents [8, 9]. Traditional methods used for the fabrication of hybrid composites include the assembly of small particles on large particles by chemical bond cross-linking [10], charge compensation [11], hydrogen-bonding interaction [7], electrostatic self-assembly [12], seeded emulsion polymerization [13] and stepwise heterocoagulation method [14] etc. Recently hydrothermal process are regarded as an alternative approach for the construction of composite particles with hybrid structure since this route has avoided the complex reaction procedures and high operating costs.

CdS is a well known II–VI semiconductor with a suitable band gap of 2.42 eV well corresponding to the solar spectrum [15, 16]. In recent years, nanoscaled CdS particles have been extensively studied for possible application in various fields due to its unique photo-chemical and photo-physical properties [17-23]. Extended applications of CdS have verified that the applicable scopes are restricted by their various inherent disadvantages, such as small specific surface area, photo-corrosion and undesirable agglomeration in the aqueous solutions during the reaction. Therefore, obtainments of the stable CdS nanoparticles to satisfy the requirement for practical use are still a great challenge. Normally, there are two strategies to improve the application of CdS nano-particle. One is to directly fabricate CdS nanoparticles using additives as stabilizers [24-25]. Another approach is to incorporate the CdS nanoparticles into a stable host matrix to form composites. Typically, CdS/rectorite [26], CdS/PMMA [27], CdS/PVA [28], CdS/polystyrene [29], and CdS/PSA [30] hybrid nano-composites have been reported.

Based on the above considerations, we report a simple strategy for fabricating novel CdS@yeast hybrid microspheres with fructus rubi-like morphology by a hydrothermal process. The novel CdS@yeast hybrid microspheres which may have integrated combined properties originating from their hybrid components, including bio-sorption or bio-molecule recognition function from yeast and the photocatalytic function with visible light response exerting by the immobilized CdS nano-particles. The as-prepared CdS@yeast composites were characterized by scanning electron microscopy (SEM), confocal laser scanning microscopy (CLSM), Energy Dispersive Spectrometer (EDS) and X-ray powder diffraction (XRD) and UV-Vis, respectively. The setting experiments were conducted to evaluate the suspension performance and stability of the hybrid microsphere in aqueous solutions. Then the cationic dye MB (methylene blue) with complex aromatic chemical structure was selected as object pollutant to examine the decolorization ability of the designed hybrid materials and the removal efficiency for MB aqueous solutions was investigated evaluated under different conditions.

2. Experimental section

2.1Preparation and characterization of fructus rubi-like CdS@yeast hybrid microspheres

All the reagents were of analytical grade purity and used as purchased without further purification. In a typical procedure, 1.0 g yeast powder was dispersed in 35 mL of distilled water (neutral pH) and 0.266 g of cadmium acetate was added. The mixture was stirred continuously at room temperature for 5.0 h and subsequently 0.24 g thioacetamide (TAA) were added. The pH value of the resulting suspension was adjusted to about pH 10 by addition of aqueous NaOH solutions. Then, the suspension was stirred vigorously for 10 min and transferred into a Teflon-lined stainless steel autoclave (50 mL capacity). The autoclave was sealed and maintained at 80°C for 6.0 h. After the reaction was completed, the resulting solid product was collected by filtration, then washed with deionized water and ethanol to remove any possible ionic species in the product, and then dried at 50 °C for 2 h.

2.2 Characterization of Samples.

The morphology of samples was studied by a JEOL-6300F Field-emission scanning electron microscope (FESEM). For fluorescent microscope study, the samples were completely sonicated before dribbling onto the tape. The dried particles were observed by confocal laser scanning microscope (CLSM, Olympus). X-ray diffraction (XRD) of the samples was determined by powder X-ray diffraction (PANalytical; -X'pert MPD Pro; CuKa). The diffuse reflectance spectra were recorded by a Varian Cary 100 Scan UV-Vis spectrophotometer. Malvern laser-velocimetry Doppler utility (Zeta sizer Nano series HT, Malvern, UK) was used for ζ-potential analysis. Fourier transform infrared (FT-IR) spectroscopy was recorded in a Bruker TENSOR 27 FTIR spectrometer.

2.3 Decolorization of methylene blue

Typically, 1.0 g of CdS@yeast hybrid composite catalysts was suspended in 100 mL of MB (1.5 mg L^{-1} initial concentration). The suspension was magnetically stirred in the dark for 120 min to establish an adsorption-desorption equilibrium prior to irradiation with a 350W Xe lamp. For decolorization on of methylene under visible light the UV part of the light was removed by a cut-off filter ($\lambda \geq 430$ nm, T=65%). Before and after irradiation, samples (3 mL) were collected at regular intervals. Each sample was centrifuged to separate the catalyst from the liquid and the supernatant was analyzed on a 722-100 spectrophotometer to determine the residual MB concentration (λ_{max}=664 nm). The samples were returned into the reactor immediately after each analysis in order to avoid the loss of catalyst dose as soon as possible in the after steps. All experiments were carried out in duplicate.

2.4 The setting performance

500 mg CdS@yeast samples, yeast, CdS nanoparticles were dispersed into 50 mL of distilled water in a vertical cylindrical burette at room temperature, respectively. At regular intervals, the falling height was determined. The sedimentation ratio *R* was measured by:

$$R = \frac{a}{a+b} \times 100\% \qquad (1)$$

a is the length of the clear fluid and *b* the length of the turbid fluid, respectively.

3. Results and Discussion

3.1 Physiochemical properties of the samples

Fig.1

FE-SEM images of samples are shown in figure 1. Figure 1(a) displays the primitive yeast cells, which are shown to be ordered ellipsoids with the length of 2.6 ± 0.4 μm and width of 2.0 ± 0.2 μm. Figure 1(b) shows a general observation of the CdS@yeast hybrid microspheres. The particles maintain the ordered ellipsoid shape of the native yeast cores and possessed relatively good mono-dispersion. The slight increasing in diameter (length = 2.6 ± 0.5 μm; width = 2.0 ± 0.3 μm) in comparison with the primitive yeast cells confirms that the CdS nanoparticles were successfully attached onto the surface of the yeast core. The higher resolution image shown in figure 1(c) indicates that all the CdS@yeast microspheres have distinct fructus rubi-like morphologies (in the insert figure 1(c)). Further magnified image of selected surface area of the CdS@yeast microsphere in figure 1(d)) verifies that the yeast surfaces are interspersed with the nano-sized CdS particles and some residual bare area on the surface of the yeast shell still remain. Additionally, figure 1(c) and (d) show that the CdS nanoparticles were attached onto the yeast cells as a monolayer, whereas a minority of them aggregated into clusters.

The insert image in figure 1(d) shows the EDS spectrum of the typical synthesized CdS@yeast composite particles. The existence of Cd and S on the particle surface can be clearly seen. As shown in the Table 1, the molar ratio of Cd to S on the surface of yeast is close to 1 which confirmed the stoichiometric formation of CdS. Here, the concentration of S element was a little more than Cd element possibly owning to S element from the yeast core, which is a kind of microorganism often containing the S element.

Table1

The confocal laser scanning microscopy and optical images of CdS@yeast samples are shown in figure 2, respectively. Each of the CdS@yeast hybrid microspheres in figure 2 (a) and (b) has exhibited clear bright blue fluorescence owing to the electronic transition of CdS nanoparticles [31]. The higher resolution image of a typical CdS@yeast specie shown in figure 2 (c) indicates that the external surface of yeast are densely and uniformly covered with the nanosized CdS nanoparticles, whereas some tiny residual bare area around the CdS nanoparticles on the surface of the yeast shell can be discerned still. In appearance, the hybrid microspheres exhibited a distinct fructus rubi-like morphology. Hereby, it is further demonstrated that the CdS nanoparticles anchored on the surface of yeast can emit fluorescence under laser stimulating. With the consideration of the yeast representing a kind of microorganism, this fluorescent characteristic also provides a possibility for their application in biological markers.

Fig.2

Figure 3 shows the XRD image of the samples. The diffraction peak at about 2θ=20° corresponds to the amorphous yeast cells. For the CdS@yeast, besides the diffraction peak from the yeast, all the other diffraction peaks are similar to the bulk CdS. For instance, the peaks at 26.5, 43.9 and 51.6^o can be indexed to the (111), (220) and (311) planes, respectively, for the cubic phase β-CdS (JCPDS01-0647) [32]. Again, CdS nanoparticles were proved to be successfully obtained through hydrothermal process and were anchored on the surface of yeast cores. No peaks from impurities were detected, indicating the high purity of the products. Meanwhile, the peaks are fairly broad, suggesting the small particle size of the as prepared CdS. According to Scherrer's equation, the average size of the CdS nanoparticles was estimated to be around 17.0 nm.

Fig.3

Figure 4 displays the UV-Vis diffuse reflectance spectra (DRS) of bare yeast, CdS and CdS@yeast hybrid particles, respectively. It is found that the bare yeast only exhibit the fundamental absorption edge at 380 nm in the ultraviolet region. The bulk CdS sample has wide photo-absorption from UV light to visible light, and the wavelength of the absorption edge is 580 nm, which could be responsible for the visible-light induced photocatalytic activity. Compared to the pure yeast and CdS nanoparticles, the CdS@yeast microspheres displayed wider absorption from ultraviolet to near-infrared region facilitating the enhanced absorption in the visible light region which accounts for almost half of the solar spectrum. Correspondingly, the color of the samples changes from brown to orange after incorporation of CdS onto the surface of yeast.

Fig.4

The sedimentation performance of CdS@yeast microspheres in aqueous solutions was also evaluated to demonstrate the unique features of CdS@yeast in comparison with CdS nanoparticles. In each experiment, yeast, CdS@yeast samples and CdS nanoparticles were dispersed in distilled water without any additional additive. From the figure 5, it is clearly observed that the CdS@yeast species have excellent suspension ability than that of CdS nanoparticles. To be more specific, the setting ratio of CdS@yeast only went down 19.6% after 330min, which is less than a quarter of that for CdS nanoparticles. The outstanding suspension stability of CdS@yeast samples is ascribed to the apparent density of yeast, as a kind of aquatic microorganisms, whose wet density ($1.09 \pm 0.008\ g \cdot cm^{-3}$) is almost equal to that of water. The analogous phenomenon also was observed in our previous study [33].

The realistic sedimentation photographs at different time are recorded as the insert images in figure 5. The lower setting ratios of samples suggest that the CdS@yeast could maintain a good dispersed state for a long time in aqueous solution. Such particular feature is beneficial to the application of CdS@yeast in removal of various pollutants in wastewater such as toxic organic, heavy metals, and dye decolorization.

Fig.5

The stability of CdS@yeast aqueous suspension was also performed in its zeta potential. The negatively charged surface of CdS@yeast (kept for 24 h at room temperature) was determined in figure 6.The zeta potential plot in figure 6 shows the average surface charge around -25.4 mV, indicating that the CdS@yeast aqueous suspension have a good stability in neutral condition because of the electrostatic repulsion effect between particles. The above-mentioned results give a further verification that CdS@yeast exhibited the important potentials for practical and long-term applications.

Fig.6

3.2 Formation of the CdS@yeast hybrid microspheres

In order to illustrate the formation mechanism of CdS@yeast via one-step hydrothermal, FT-IR spectra of yeast cells, pure CdS and CdS@yeast composites were recorded, respectively, as shown in figure 7. The characteristic adsorption peaks of bare yeast in figure 7 (a) at 3375.39, 2925.98, 1652.97 and 1074.37 cm^{-1} can be ascribed to the O–H stretching vibration, CH_2 asymmetric stretching vibration, amide group and C-O stretching vibration, separately [34-38]. Compared with pure yeast, the characteristic peaks of O–H in the spectrum of fructus rubi-like Cd^{2+}@yeast composites shifted to 3386.96 cm^{-1} and the C-O stretching vibration moved to 1076.96 cm^{-1}. These shifts imply that the hydroxyl and carboxyl of yeast have some kind of interaction with Cd^{2+} ions to form intermediate product Cd^{2+}@yeast. Meanwhile, from the spectrum of CdS@yeast, it can be seen that all the characteristic bands of O-H, CH_2, amide group and C-O showed certain degree of shift compared to the pure yeast and Cd^{2+}@yeast.

Fig.7

Accordingly, above observations suggest that the abundant functional groups on the surface of the pristine cells played an important role in the formation of the fructus rubi-like CdS@yeast hybrid microspheres. In the case of pristine yeast cells, the cell wall contains an appreciable amount of complex organic compounds and polymers such as glucan (28.8% *w/w*), mannan (31%), proteins (13%), lipids (8.1%) chitin and chitosan (2%) and inorganic ions [39]. Hence, these diverse chemical substances in the cell wall would provide a wide range of hydrophilic anionic groups including OH^-, $-CONH^-$, $-COO^-$, and $-OPO_3^{2-}$ [39], as also demonstrated by the FT-IR spectra in figure 7. These hydrophilic groups on the yeast cell-wall provide ideal binding sites for the anchoring of the Cd^{2+} ion. Thereafter, abundant Cd^{2+} ions pre-absorbed on the walls of the yeast cells will form the CdS colloids on the surface of the yeast cells during the hydrothermal processes in the presence of TTA, which gradually grow into the CdS@yeast microspheres with a fructus rubi-like morphology. These processes can be partly explained by the traditional combined sorption–micro-precipitation mechanism [40]. The possible fabrication mechanism of the CdS@yeast is schematically illustrated in figure 8.

Fig.8

3.3 Photocatalytic test

The fructus rubi-like CdS@yeast microspheres exhibiting a partially covered surface of yeast cell cores could provide unique properties for removal of water pollutants. The inlaid yeast surfaces might facilitate bio-sorption of organic species while the outer CdS nanoparticles can be responsible for the photocatalytic degradation of the species. The environmental application of the fructus rubi-like CdS@yeast hybrid microspheres is demonstrated for the decolourization of MB aqueous solutions as model organic dye. The results are shown in figure 9.

Fig.9

Near absorption-desorption equilibrium was established through two hours in dark preceding the irradiation of the dyes solutions. In figure 9 almost the same temporal absorption profiles by the naked yeasts and CdS@yeast microspheres for MB aqueous solutions can be seen with the absence of Xe lamp illuminating, which imply that the attachments of CdS nanoparticles onto yeast surface have not serious effects on the adsorption of MB molecular. Such agreements can also be affirmed by contrasting the pseudo first-order kinetic constant k_1 in dark under above-mentioned different conditions. The results were listed in table 2. As seen in table 2, the extremely slight discrepancy of pseudo first-order kinetic constant k_1 suggest that the adsorbent of bare yeast and CdS@yeast microspheres have a nearly similar absorption capability for the MB molecular in dark. In theory, the favourable absorption ability by the primitive yeasts for MB molecular can be attributed to the negatively charged surface [41], which favours the capture of the cationic MB dye through electrostatic attraction or hydrogen bond interaction. Interestingly, the succedent occupation of absorption sites through anchoring CdS nanoparticles onto the surface of yeast did not lead to a serious descent of adsorption efficiency for MB aqueous solutions compared to that of naked yeast. The real cause lies in that the CdS nanoparticles on the surface of yeast were also negatively charged in neutral condition [42-43], which compensating for the loss of active absorption sites from the invasion of CdS nanoparticles.

With Xe lamp as simulated light, the experiments of decolourization of MB aqueous solutions were carried out under UV light (λ>300 nm) and visible light (λ>430), respectively. With the help of light exciting the decolourization of MB aqueous solutions should be governed by the absorption and photocatalysis synchronously. The former one could transfer the MB molecular from aqueous solutions to the vacant sites of CdS@yeast surface by absorption function, while the latter one could decompose the MB molecular by photocatalytic function. Usually these two procedures take place simultaneously in the presence of CdS@yeast microspheres under irradiation. As a result, it is a cooperative effect that results in the decrease of MB concentration with the irradiation time prolonged. The temporal curves of MB removal efficiency under the light irradiating were also shown in figure 9. It could be seen in figure 9 (a) that MB aqueous solutions is barely photolyzed by the UV irradiation alone, whereas approximately 44.4% of MB was removed from the aqueous solutions by bio-sorption on the naked yeast in figure 9 (b). With the presence of the fructus rubi-like CdS@yeast microspheres under UV light irradiation, approximately 61.2% of MB decolorization efficiency was accomplished in figure 9 (d). Eliminating 300~430 nm light band through a cutoff filter from UV light (changed to visible light) deliberately has turned the decolorization efficiency down to 57.5% in figure 9 (c). Obviously, attachment of CdS nanoparticles onto the surface of yeast and illuminating with UV light are beneficial for the decolorization of dye commonly. The inflection at time zero provides further assertive evidence of the MB decomposition. Moreover, the higher removal efficiency of MB molecular from the aqueous solutions in dark in comparison with in the light illumination conditions suggests that the bio-sorption function of yeast seems act as predominant roles for the removal of MB.

Fig.10

To further illustrate the role of CdS nanoparticle and the illumination of the simulated sunlight in the photocatalytic decolourization, the experimental data were fitted by applying a pseudo first order model as expressed by Eq. (2), which is well established for the photocatalytic experiments when the pollutant is in the millimolar concentration range [42].

$$\ln\frac{C_t}{C_0} = k \cdot t \tag{2}$$

Where C_0 is the initial concentration and C_t is the concentration of MB aqueous solutions at the time t, k is pseudo first-order kinetic constant, respectively. Figure 10 shows the comparison of pseudo first-order plots for the decolorization of MB aqueous solutions by different methods. From the figure 10 we could see that all the plots of irradiation time t versus the $\ln(C_t/C_0)$ displayed a nearly straight line. The regressed pseudo first-order kinetic constant k_2 and adj. R-Square R^2 were summarized in table 2. As shown in table 2 the rate constant k_2 of the photolysis alone is closed to zero for the duration of the test. Moreover, the independent absorption by naked yeast for 6.0 h has the lowest rate constant (k_2= 1.4×10^{-3} g/mg·min), whereas the CdS@yeast hybrid microspheres under the illumination of the UV light has the highest rate constant (k_2 = 12.0×10^{-3} g/mg·min), which is almost ten times of that for the naked yeast at the same conditions. In contrast, irradiation with visible light has resulted in a smaller rate constant (k_2 = 6.61×10^{-3} g/mg·min) compared to CdS@yeast under UV light. Clearly, the attachment of CdS nanoparticles on the surface of yeasts and the illumination with UV light had a great significant influence on the removal rate of MB aqueous solutions.

Table 2

These results suggest that our prepared CdS@yeast composites can be effective for the removal of MB dye. The integration of bio-sorption by the yeast with photocatalysis by the CdS nanoparticles attached on the yeast cells has showed a combined function in the removal of the dye from the aqueous solutions. More specifically, the removal of MB via bio-sorption of the yeast core surface is preserved by keeping the adsorption sites unsaturated through the decomposition of the molecules by CdS photo-catalysis. In return, the simultaneous bio-sorption of MB molecule via the reborn surfaces of the yeast core provides a continuous supply of substrate to the CdS nanoparticles for its destruction by photocatalysis. Thus, the bio-sorption performance of yeast and the photocatalytic performance of the attached CdS nanoparticles have been integrated as a novel property for the fructus rubi-like CdS@yeast composites.

4. Conclusions

In summary, a strategy based on the single-step hydrothermal process was successfully developed to fabricate stable fructus rubi-like CdS@yeast hybrid microspheres. In this method, the pre-existence of functional groups inherited from the hydrophilic cell wall of microbial cells are responsible for the anchoring of CdS guest nanoparticles onto yeast cells host surfaces. The potential applications of these new composites were demonstrated for the decolourization of methylene blue from wastewater. The enhancement of the removal efficiency is attributed to the integrated properties of bio-sorption and photocatalysis originating from their constituent components. Moreover, the obtained CdS@yeast samples have good stability and outstanding suspension property, suggested their great potentials in the treatment of the toxic organic pollutants.

Acknowledgments

This work was financially supported by National Natural Science Foundation of China (No.21176031), China Postdoctoral Science Special Foundation, Scientific Research Foundation for the Returned Overseas Chinese Scholars and Fundamental Research Funds for the Central Universities (No. 2013G2291015).

References

[1] Hongfen Ji, Siping Wang, Xinlin Yang. Preparation of polymer/silica/polymer tri-layer hybrid materials and the corresponding hollow polymer microspheres with movable cores, Polymer, 2009, 50: 133 – 140.

[2] Yudong Zhang, Sangho Lee, Mitra Yoonessi, Kaiwen Liang, Charles U. Pittman. Phenolic resin–trisilanolphenyl polyhedral oligomeric silsesquioxane (POSS) hybrid nanocomposites: Structure and properties, Polymer, 2006, 47:2984–2996.

[3] M. Agrawal, A. Pich, N.E. Zafeiropoulos, S. Gupta, J. Pionteck, F. Simon, M.Stamm, Polystyrene – ZnO composite particles with controlled morphology, Chemistry of Materials, 2007, 19:1845 – 1852.

[4] Wenlong Cheng, Shaojun Dong, Erkang Wang, Two- and three-dimensional Au nanoparticle/CoTMPyP self-assembled nanostructured materials: Film structure, Tunable electrocatalytic activity, and Plasmonic properties, Journal of Physical Chemistry B, 2004, 108(50):19146 – 19154.

[5] Shaojun Guo, Shaojun Dong, Erkang Wang. Raspberry-like hierarchical Au/Pt nanoparticle assembling hollow spheres with nanochannels: an advanced nanoelectrocatalyst for the oxygen reduction reaction, Journal of Physical Chemistry C, 2009, 113(14) :5485 – 5492.

[6] Lianbin Zhang, Yang Li, Junqi Sun, Jiacong Shen, Mechanically stable antireflection and antifogging coatings fabricated by the layer-by-layer deposition process and postcalcination, Langmuir, 2008, 24(19): 10851 – 10857.

[7] Hongli Liu, Dan Wang, Xinlin Yang, Preparation of polymer@titania raspberry-like core – corona composite via heterocoagulated self-assembly based on hydrogen-bonding interaction Colloids and

Surfaces A: Physicochemical and Engineering Aspects, 2012, 397 :48－58.

[8] Wang Xin, Akagi Takami, Akashi Mitsuru, Baba Masanori, Development of core－corona type polymeric nanoparticles as an anti-HIV-1 vaccine, Mini-Reviews in Organic Chemistry, 2007, 4:51－59.

[9] Takami Akagia, Masanori Babab, Mitsuru Akashia, Preparation of nanoparticles by the selforganization of polymers consisting of hydrophobic and hydrophilic segments: potential applications, Polymer, 2007, 48:6729－6747.

[10] Urara Hasegawa, Shin-ichi Sawada, Takeshi Shimizu, Tsunao Kishida, Eigo Otsuji, Osam Mazda, Kazunari Akiyoshi. Raspberry-like assembly of cross-linked nanogels for protein delivery, Journal of Controlled Release, 2009, 140(3): 312–317.

[11] Guoliang Li, Xinlin Yang, Feng Bai, Wenqiang Huang. Raspberry-like composite polymer particles by self-assemble heterocoagulation based on a charge compensation process, Journal of Colloid and Interface Science, 2006, 297(2): 705–710.

[12] Bo Bai, Natalia Quici, Ziyan Li, Gianluca Li Puma, Novel one step fabrication of raspberry-like TiO_2@yeast hybrid microspheres via electrostatic-interaction-driven self-assembled heterocoagulation for environmental applications, Chemical Engineering Journal, 2011,170: 451－456.

[13] Shan Shi, Limin Zhou, Tao Wang, Lina Bian, Yantao Tang, Shin-ichi Kuroda, Preparation of raspberry-like poly(methyl methacrylate) particles by seeded dispersion polymerization, Journal of Applied Polymer Science, 2011, 120: 501－508.

[14] M. Okubo, Y. Lu, Production of core-shell composite polymer particles utilizing the stepwise heterocoagulation method, Colloids and Surfaces A: Physicochemical and Engineering Aspects,

1996, 109: 49–53.

[15] B.S. Zou, R.B. Little, J.P. Wang, M.A. El-Sayed. Effects of different capping environments on the optical properties of CdS nanoparticles in reverse micelles, International Journal of Quantum Chemistry, 1999,72: 439 – 450.

[16] A.P. Alivisatos,. Semiconductor clusters, nanocrystals, and quantum dots, Science, 1996,271: 933 – 937.

[17] V.L. Colvin, M.C. Schlamp, A.P. Alivisatos. Light-emitting-diodes made from cadmium selenide nanocrystals and a semiconducting polymer, Nature, 1994, 370:354–357.

[18] Ting Yang, Mengmeng Lu, Xiaoli Mao, Wenhong Liu, Lei Wan, Shiding Miao, Jinzhang Xu. Synthesis of CdS quantum dots (QDs) via a hot-bubbling route and co-sensitized solar cells assembly, Chemical Engineering Journal, 2013,225: 776 – 783.

[19] Willner I, Willner B. Functional nanoparticle architectures for sensoric, optoelectronic and bioelectronic applications, Pure Appl. Chem., 2002, 74(9):1773–1783.

[20] Keiichi Sato, Yasuhiro Tachibana, Shinya Hattori, Taeko Chiba, Susumu Kuwabata, Polyacrylic acid coating of highly luminescent CdS nanocrystals for biological labeling applications, Journal of Colloid and Interface Science, 2008, 324(1–2):257–260.

[21] Yoonmook Kang, Donghwan Kim. Enhanced optical sensing by carbon nanotube functionalized with CdS particles, Sensors and Actuators A: Physical, 2006, 125(2): 114–117.

[22] H.M. Yang, C.H. Huang, X.W. Li, R.R. Shi, K. Zhang, Luminescent and photocatalytic properties of cadmium sulfide nanoparticles synthesized via microwave irradiation, Mater. Chem. Phys., 2005, 90: 155-158.

[23] Yuming Guo, Xiaoman Shi, Jie Zhang, Qilong Fang, Lin Yang ,Fangfang Dong, Kui Wang. Facile

one-pot preparation of cadmium sulfide quantum dots with good photocatalytic activities under stabilization of polar amino acids, Materials Letters, 2012, 86: 146–149.

[24] Chanu TI, Negi DPS. Synthesis of histidine-stabilized cadmium sulfide quantum dots: study of their fluorescence behaviour in the presence of adenine and guanine, Chem. Phys. Lett., 2010, 491: 75-79.

[25] Yuming Guo, Lingling Wang, Lin Yang, Jie Zhang, Lili Jiang, Xiaoming Ma, Optical and photocatalytic properties of arginine-stabilized cadmium sulfide quantum dots, Materials Letters, 2011,65: 486 – 489.

[26] Jiangrong Xiao, Tianyou Penga, Ke Dai, Ling Zan, Zhenghe Peng. Hydrothermal synthesis, characterization and its photoactivity of CdS/Rectorite nanocomposites, Journal of Solid State Chemistry, 2007, 180: 3188–3195.

[27] Li Chen, Jia Zhu, Qing Li, Su Chen, Yanru Wang. Controllable synthesis of functionalized CdS nanocrystals and CdS/PMMA nanocomposite hybrids, European Polymer Journal, 2007, 43: 4593–4601.

[28] Hongmei Wang, Zhe Chen, Pengfei Fang, Shaojie Wang. Synthesis, characterization and optical properties of hybridized CdS-PVA nanocomposites, Materials Chemistry and Physics, 2007, 106: 443–446.

[29] Xinjian Cheng, Qiang Zhao, Yingkui Yang, Sie Chin Tjong, Robert K.Y. Li. A facile method to prepare CdS/polystyrene composite particles, Journal of Colloid and Interface Science, 2008, 326: 121–128.

[30] Chunnian Chen, Chunling Zhu, Linyun Hao, Yuan Hu, Zuyao Chen. Preparation and characterization of the CdS/PSA core-shell ‘‘egg’’, Inorganic Chemistry Communications, 2004,

7:2004 322–326.

[31] Yun-Jie Yang , Xia Tao , Qian Hou, Jian-Feng Chen, Fluorescent mesoporous silica nanotubes incorporating CdS quantum dots for controlled release of ibuprofen, Acta Biomaterialia, 2009, 5: 3488-3496.

[32] Powder diffraction file. Swarthmore, PA: JCPDS International Center for Diffraction Data, 1982, No. 10–454.

[33] Lan Chen, Bo Bai. Facile preparation of phosphotungstic acid-impregnated yeast hybrid microspheres and their Photocatalytic performance for decolorization of azo Dye, International Journal of Photoenergy, 2013, 406158:1-9.

[34] Joris, C.H.Amberg. The nature of deficiency in nonstoichiometric hydroxyapatites II spectroscopic studies of calcium and strontium hydroxyapatites [J]. Journal of Chemical Physics, 1971, 75(20): 3172–3178.

[35] Michael Beekes, Peter Lasch, Dieter Naumann, Analytical applications of fourier transform-infrared (FT-IR) spectroscopy in microbiology and prion research. Veterinary Microbiology, 2007, 123(4): 305-319.

[36] KC Blakeslee, RA Condrate. Vibration spectra of hydrothermal prepared hydroxyapatites. J. Am. Ceram. Soc., 1971, 54(11): 559–563.

[37] KJ Rothschild, NA Clark. Anomalous amide I infrared absorption of purple membrane [J], Science, 1979, 204(4390): 311-312.

[38] R.A. Nyquist, R.O. Kagel. Infrared spectra of inorganic compounds [M], Academic Press, New York, London, 1971.

[39] Jianlong Wang, Can Chen. Biosorbents for heavy metals removal and their future, Biotechnology

Advances, 2009, 27: 195-226.

[40] A.B. Ariff, M. Mel, M.A. Hasan. M.I.A. Karim. The kinetics and mechanism of lead (II) biosorption by powderized Rhizopus oligosporum, World. J. Microb. Biot., 1999, 15: 291-298.

[41] A. Bingol, H. Ucun, Y.K. Bayhan, A. Karagunduz, A. Cakic, B. Keskinler, Removal of chromate anions from aqueous stream by a cationic surfactant-modified yeast, Bioresource. Technol., 2004, 94: 245-249.

[42] Lei Ge, Jing Liu, Efficient visible light-induced photocatalytic degradation of methyl orange by QDs sensitized CdS-Bi_2WO_6 Applied Catalysis B: Environmental, 2011, 105: 289-297.

[43] Egon Matijevic, D.M. Wilhelmy. Preparation and properties of monodispersed spherical colloidal particles of cadmium sulfide, Journal of Colloid and Interface Science, 1982, 86: 476–484.

[44] Xiaojiao Zhang, Shiwei Lin, Jianjun Liao, Nengqian Pan, Danhong Li, Xiankun Cao,Jianbao Li, Uniform deposition of water-soluble CdS quantum dots on TiO_2 nanotube arrays by cyclic voltammetric electro deposition: Effectively prevent aggregation and enhance visible-light photocatalytic activity, Electrochimica Acta, 2013, 108: 296-303.

Figure captions

Fig.1. SEM images of (a) naked yeast, (b) overall observation of fructus rubi-like CdS@yeast microspheres, (c) close observation of (b), (d) EDS spectra for the selected square (within dotted line) in (c)

Fig.2. Confocal laser scanning microscopy (a), (b), (c) and optical image (d) of CdS@yeast microspheres

Fig.3. XRD patterns of the yeast, fructus rubi-like CdS@yeast samples and CdS nanoparticles, respectively

Fig.4. UV-Vis spectra of bare yeast, CdS and CdS@yeast hybrid microspheres, respectively

Fig.5. Settling curves of pure yeast, CdS nanoparticles and CdS@yeast microspheres, respectively

Fig.6. Zeta potential plot of the CdS@yeast aqueous suspension in neutral conditions

Fig.7. FT-IR spectra of (a) pristine yeast, (b) Cd^{2+}@yeast, (c) CdS@yeast microspheres

Fig.8. Mechanism for the formation of the CdS@yeast microspores with fructus rubi-like structures

Fig.9. Temporal changes in the relative concentration of MB due to: (a) UV photolysis, (b) UV photolysis and adsorption by the naked yeast, (c) decolorization by the CdS@yeast microspheres with visible light (d) decolorization by the CdS@yeast microspheres with UV light

Fig.10. Pseudo first-order plots for the decolorization of MB by (a) UV photolysis, (b) UV photolysis and adsorption by the naked yeast, (c) decolorization by the CdS@yeast microspheres with visible light, (d) decolorization by the CdS@yeast microspheres with UV light

Fig.1

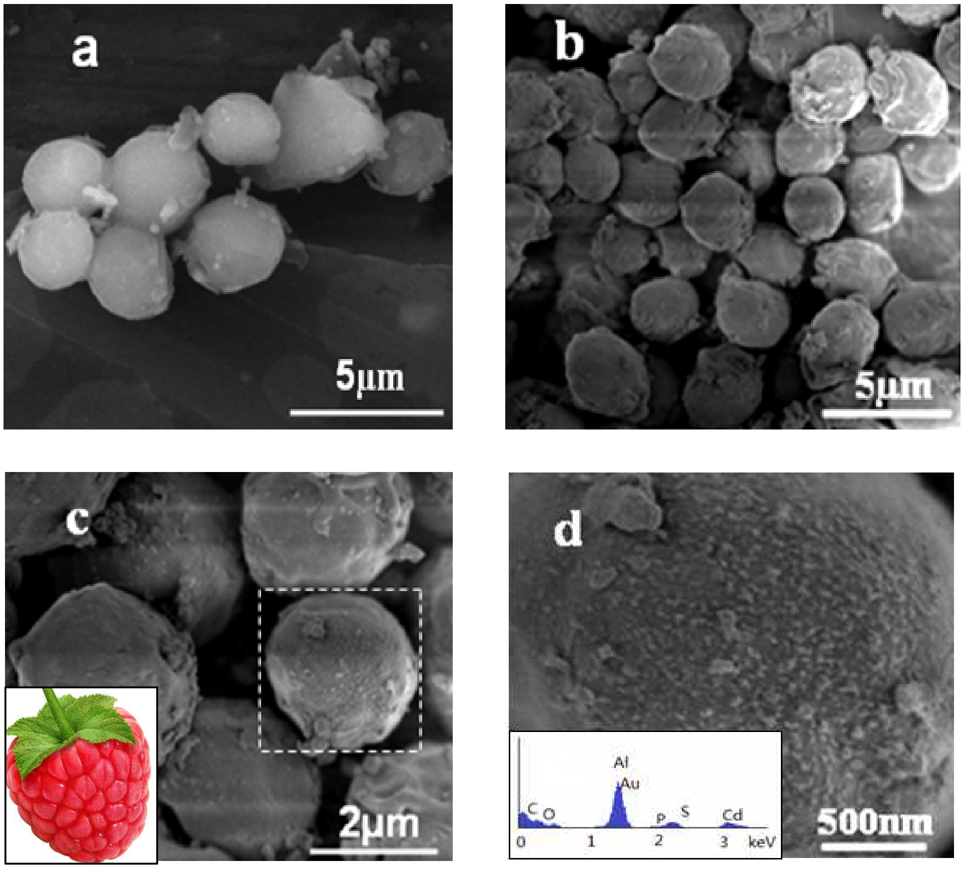

Fig.2

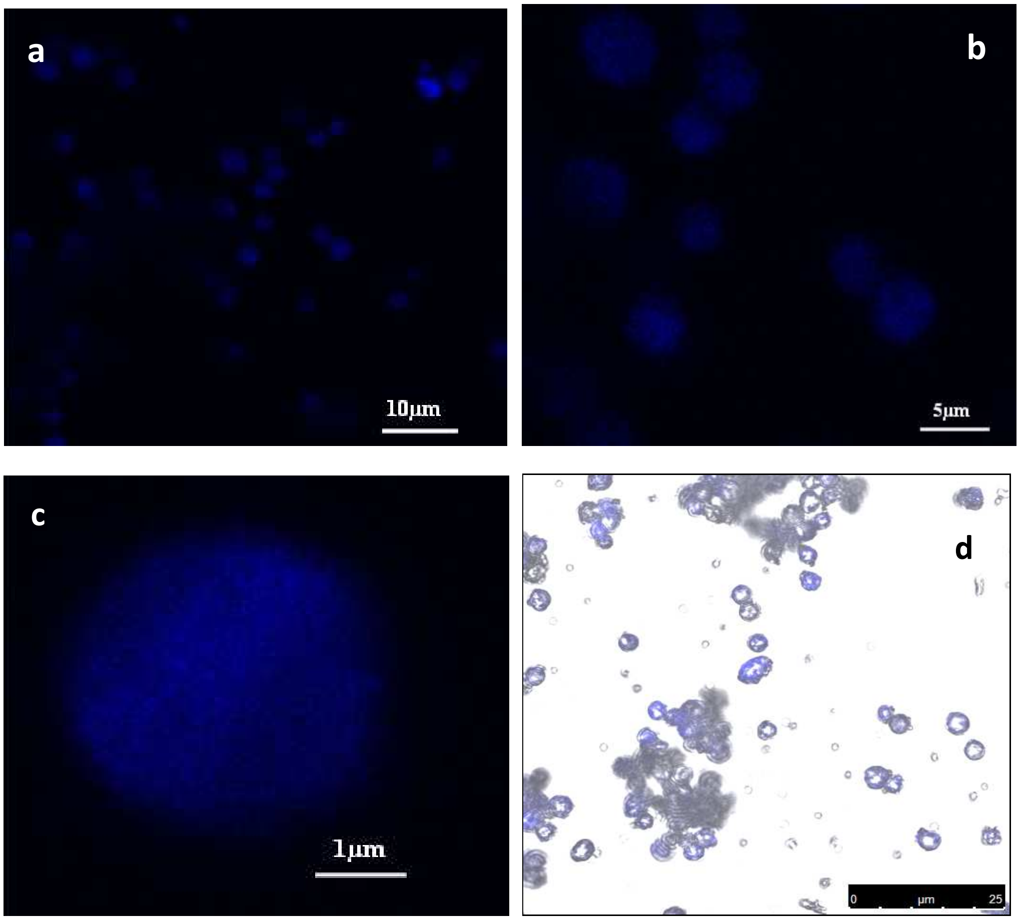

Fig.3

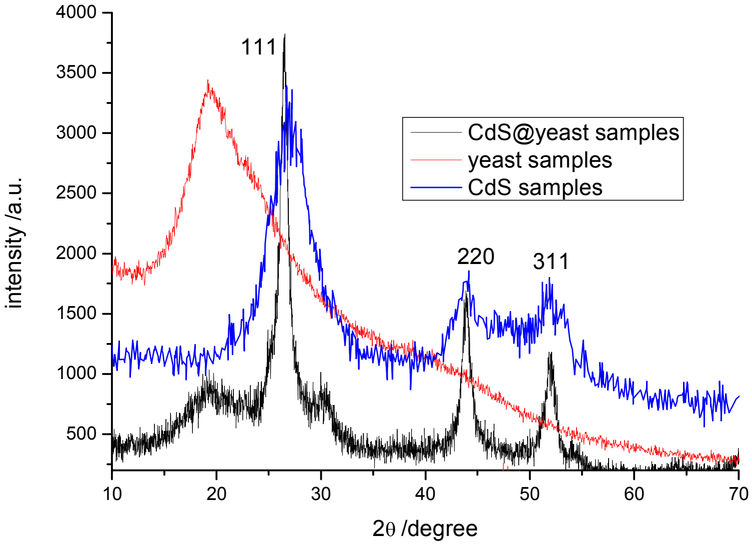
4000
3500
3000
2500
2000
1500
1000
500
intensity /a.u.
10
20
30
40
50
60
70
2θ /degree
111
220
311
CdS@yeast samples
yeast samples
CdS samples

Fig.4

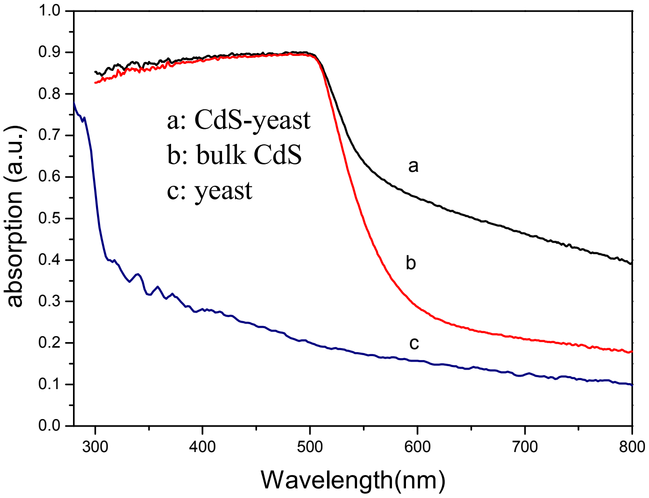
a: CdS-yeast
b: bulk CdS
c: yeast
a
b
c
absorption (a.u.)
Wavelength(nm)
0.0
0.1
0.2
0.3
0.4
0.5
0.6
0.7
0.8
0.9
1.0
300
400
500
600
700
800

Fig.5

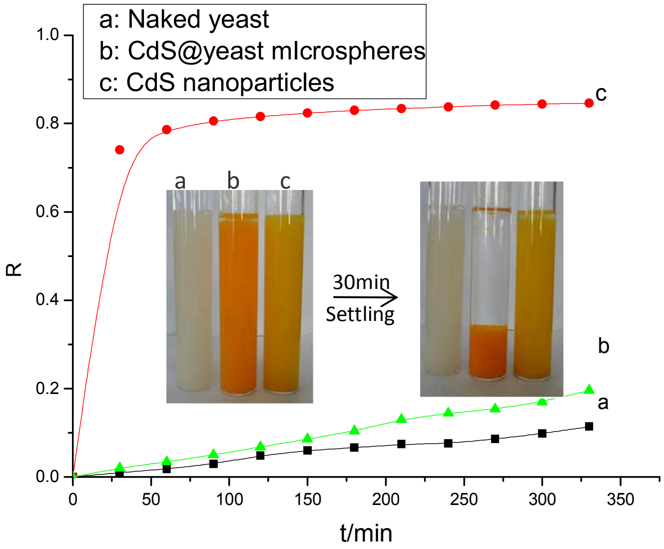
a: Naked yeast
b: CdS@yeast mIcrospheres
c: CdS nanoparticles
R
t/min
1.0
0.8
0.6
0.4
0.2
0.0
0
50
100
150
200
250
300
350
a
b
c
30min
Settling

Fig.6

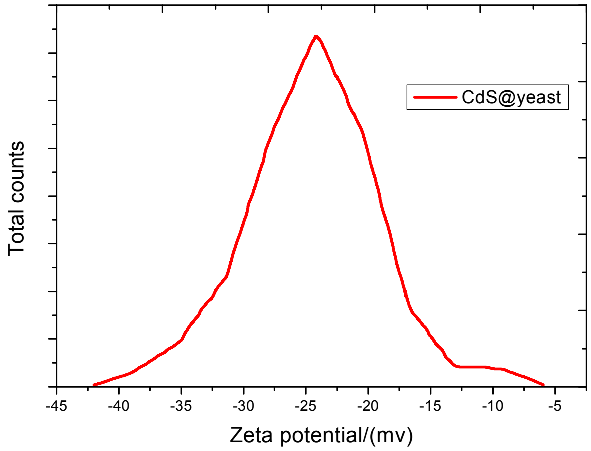
Total counts
CdS@yeast
-45
-40
-35
-30
-25
-20
-15
-10
-5
Zeta potential/(mv)

Fig.7

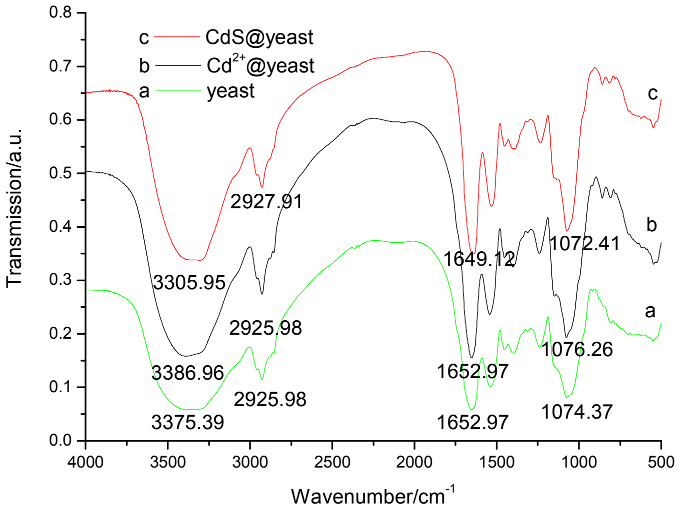
c CdS@yeast
b Cd^{2+}@yeast
a yeast
Transmission/a.u.
Wavenumber/cm^{-1}
0.0
0.1
0.2
0.3
0.4
0.5
0.6
0.7
0.8
4000
3500
3000
2500
2000
1500
1000
500
c
b
a
2927.91
3305.95
1649.12
1072.41
2925.98
3386.96
1652.97
1076.26
2925.98
3375.39
1652.97
1074.37

Fig.8

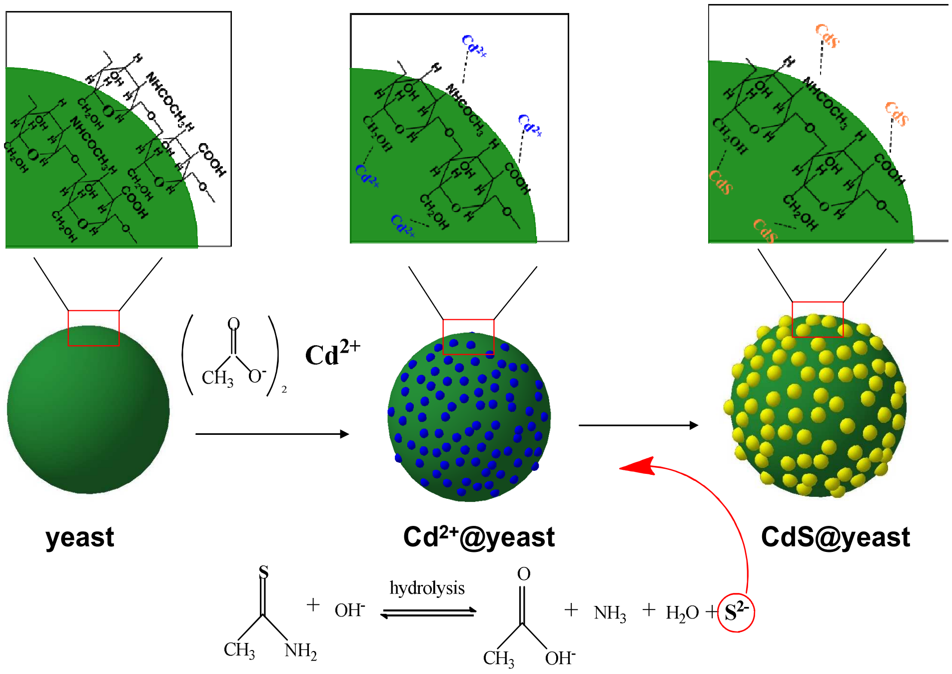
NHCOCH₃
CH₂OH
COOH
OH
Cd²⁺
CdS
Cd²⁺
yeast
Cd²⁺@yeast
CdS@yeast
S
CH₃
NH₂
+ OH⁻
hydrolysis
O
CH₃
OH⁻
+ NH₃ + H₂O + S²⁻

Fig.9

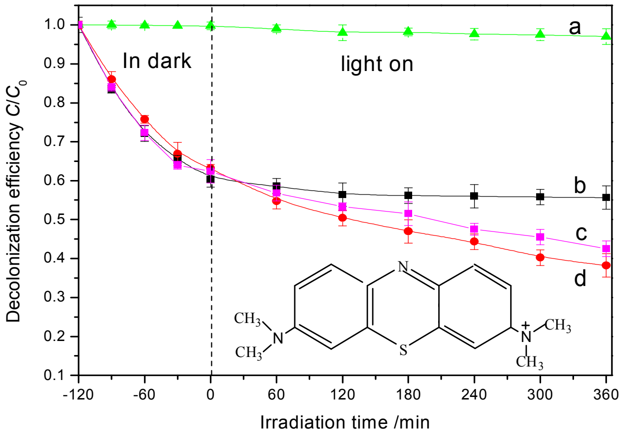
Decolonization efficiency C/C_0
1.0
0.9
0.8
0.7
0.6
0.5
0.4
0.3
0.2
0.1
-120
-60
0
60
120
180
240
300
360
Irradiation time /min
In dark
light on
a
b
c
d
N
S
CH_3
N
CH_3
$\overset{+}{N}$
CH_3
CH_3

Fig.10

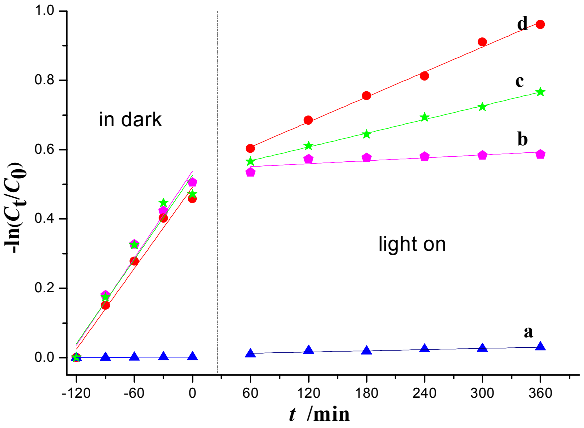

1.0
0.8
0.6
0.4
0.2
0.0
$-\ln(C_t/C_0)$
in dark
light on
d
c
b
a
-120
-60
0
60
120
180
240
300
360
t /min

Table captions

Table 1 The element distribution on the surface of CdS@yeast microsphere

Table 2 Pseudo first-order kinetic constant k_1 (in dark), k_2 (light on) and Adj. R-Square R^2 for decolorization of MB under different conditions

Table1

Element	C	O	Al	P	S	Cd	Au
Weight percentage	42.71	16.40	32.01	0.56	1.49	3.64	3.19
Atom percentage	60.47	17.43	20.18	0.31	0.79	0.55	0.28

Table2

Name	Decolorization of MB by UV photolysis alone	Decolorization of MB by yeast absorption and UV photolysis	Decolorization of MB by CdS@yeast with visible light	Decolorization of MB by CdS@yeast with UV light
k_1 (g/mg·min)	2.20×10^{-5}	4.18×10^{-3}	4.05×10^{-3}	3.90×10^{-3}
R^2	0.867	0.964	0.930	0.972
k_2 (g/mg·min)	5.9×10^{-5}	1.40×10^{-3}	6.61×10^{-3}	12.0×10^{-3}
R^2	0.856	0.601	0.997	0.994